Preparation and characterization of the defect–conductivity relationship of Ga-doped ZnO thin films deposited by nonreactive radio-frequency–magnetron sputtering

M. Lalanne, J.M. Soon, A. Barnabé,[a] L. Presmanes, I. Pasquet, and Ph. Tailhades
Université de Toulouse UPS-INP-CNRS, Institut Carnot CIRIMAT, 31062 Toulouse Cedex 4, France

Ga-doped ZnO (ZnO:Ga) thin films were prepared by radio-frequency–magnetron sputtering on conventional glass substrates at room temperature. The structural, electrical, and optical properties of these films as a function of argon pressure and film thicknesses were studied. All the films crystallized with the hexagonal wurtzite structure. The x-ray diffraction studies show that the ZnO:Ga films are highly oriented with their crystallographic *c*-axis perpendicular to the substrate. We discuss a methodology of using a "standardized platform" for comparison of samples deposited at different pressures, which provides an insight into the defect–resistivity relationship of each sample with respect to their microstructure. After the first annealing, the electrical properties of the films are dependent on the atmosphere used during postdeposition annealing treatment. A resistivity of $2.5 \times 10^{-3}\ \Omega \cdot$ cm was obtained after vacuum annealing, and the films became an insulator after air annealing. The reproducibility of this treatment was verified. The average transmittance of all ZnO:Ga thin films is more than 85% in the visible range.

I. INTRODUCTION

Zinc oxide is used in a variety of technical applications, including porcelain enamels, heat resisting glass, spacecraft protective coatings, healing ointments, optical waveguides, in piezoelectric materials, semiconductor devices, as a catalyst, as an activator in vulcanization, as an additive for rubber and plastics, pigment in paints with ultraviolet (UV)-protective and anti-fungistatic properties, and even as a constituent in cigarette filters.[1] Devices based on semiconductor ZnO thin films are potentially interesting and often used for optoelectronics in the UV as well as for transparent electronics; thin-film solar cells[2] and flat panel displays[3,4] are typical applications of this material. Appropriately doped ZnO may be highly transparent and conductive and can therefore be used as substitutes for indium tin oxide (ITO) in transparent conducting oxide (TCO) applications. This broad versatility is the result of the intrinsic properties of zinc oxide, some of which are unique, just like its surface properties. ZnO is an n-type semiconductor with a wide direct band gap energy of 3.37 eV at room temperature. The electrical conductivity of this material is mainly due to intrinsic defects such as interstitial zinc atoms and oxygen vacancies. Its electrical conductivity can be increased by doping with group III elements as well as by annealing treatments in controlled atmospheres. An additional aspect of ZnO is the possibility to prepare ZnO nanopillars with a high degree of *c*-axis orientation by self-organization. These properties have boosted tremendous research efforts worldwide.[5]

Many deposition techniques such as reactive sputtering, spray pyrolysis, chemical vapor deposition, and sol-gel have been reported to produce zinc oxide thin films. However, most of these techniques require intentional heating at moderate temperatures to obtain good electrical properties,[6] or they suffer from undesirable process-related heating that cannot be avoided. In addition, in the case of deposition on glass substrates coated with color filters made of resin, and on plastic substrates such as polycarbonate sheets, the films must be deposited at substrate temperatures lower than 250 and 140 °C, respectively. Hence, it is necessary to prepare conductive films with such resistivity at a low substrate temperature. Nonreactive radio frequency (rf) magnetron sputtering is one of the most appropriate techniques for the preparation of such ZnO based materials: it can operate under reasonably low oxygen partial pressures and with a low substrate temperature.[7] Its versatility in terms of variable apparatus configurations and deposition parameters allows fine control of the defect chemistry of ZnO thin films. Consequently, this technique can be used to fabricate ZnO-based thin films with high optical transmittance and a low electrical conductivity.

In general, Ga-doped zinc oxide (ZnO:Ga) is less studied than Al-doped zinc oxide (ZnO:Al) mainly because of the higher price of gallium compared with aluminum.

[a]Address all correspondence to this author.
e-mail: barnabe@chimie.ups-tlse.fr

Yet, gallium is better for most applications because it is less reactive and more resistant to oxidation than aluminum. Moreover, the covalent bond lengths of Ga–O and Zn–O are estimated to be 1.92 and 1.97 Å, respectively, using their atomic radii.[8–10] This similarity is an advantage since it creates only a small deformation of the ZnO lattice even in the case of high concentration Ga doping. On the other hand, ZnO doped with indium, also from group V of the periodic table, has been studied.[11] While the general trend in electrical behavior of ZnO:In is similar to that of ZnO:Ga, the change in ZnO:Ga is greater, hence offering a larger window for manipulation to achieve low electrical conductivity.

In this paper, the morphological, electrical, and optical properties of Ga-doped ZnO thin films deposited by nonreactive rf sputtering are studied in detail. Several articles have already reported the effect of the pressure deposition on the microstructure and the physical properties of doped ZnO thin films deposited by rf sputtering.[8,12] However, in this paper, we show that by repetitive cycling in air and in vacuum, the resistivity of the film was found to cycle reversibly between an insulator and $2.5 \times 10^{-3}\ \Omega \cdot$ cm, respectively. We discuss a methodology of comparing the resistivity of samples deposited at different pressures using a "standardized platform," which provides an insight into the defect–resistivity relationship for the samples. The average transmittance of the ZnO:Ga thin film is more than 85% in the visible range.

II. EXPERIMENTAL

Gallium-doped zinc oxide thin films were deposited using a nonreactive rf-magnetron sputtering technique on conventional glass substrates. The deposition system used was an Alcatel A 450 conventional planar system. A ZnO ceramic target doped with 2 at.% Ga was pressed and sintered at 1000 °C for 5 h in air. The relative density of the target was about 80%, and x-ray diffraction showed a pure wurtzite phase. Magnetron sputtering deposition was carried out at room temperature with the rf sputtering power maintained at a constant of 50 W. The target-to-substrate distance was fixed at 5 cm. The argon pressure was varied from 0.3 to 1.5 Pa. Films with different thicknesses ranging from 15 to 450 nm were deposited.

The film thickness was measured by a surface profilometer (Dektak 3030ST). The electrical resistivity was measured using classical four-point probe measurements and expressed in area resistivity, $R\Upsilon$ to correct for the form factor of each sample. The carrier concentration and carrier mobility were determined from Hall effect measurements using the Van der Pauw method with an applied external field of 0.51 T. The optical transmittance was measured using a UV-vis spectrometer (Cary 1E Varian) in the wavelength range of 350 to 850 nm. X-ray diffraction (XRD) phase analyses were done in the θ–2θ mode using a Bruker D4 diffractometer equipped with a Cu target (Cu Kα radiation; $\lambda = 1.5406$ Å) and a Seifert XRD3003TT diffractometer in grazing incident mode. For the analysis of crystallite size using the Scherrer formula, all raw XRD data were corrected for the instrumental contributions to the full width at half-maximum (FWHM), which has been measured using a standard sample of Al_2O_3 (Reference: SRM 1976) certified by the National Institute of Standards and Technology (NIST). Atomic force microscope (AFM; Nanoscope III Dimension 3000), scanned over a surface area of 1 μm^2, and field emission gun scanning electron microscope (FEG SEM; JEOL JSM 6400) were used for determination of the grain size, roughness, and microstructure of the films. The specimens for cross-sectional transmission electron microscopy (TEM) analysis were deposited on a Si substrate and studied with a JEOL 2100F field emission gun transmission electron microscope operating at 200 kV and equipped with a scanning TEM (STEM) system.

Annealing of the as-deposited samples was performed always in a sequence starting from vacuum annealing, followed by the air annealing, and repeated if necessary following this sequence. Regardless of the atmosphere used, the sample was annealed from room temperature (25 °C) to 400 °C over a period of 120 min (3.1 °C/min), where it is allowed a dwell time of 60 min, before it is allowed to cool to room temperature again over 120 min.

III. RESULT AND DISCUSSION

XRD measurements indicate that for all the deposition pressures, the as-deposited ZnO:Ga films are polycrystalline with the hexagonal wurtzite structure and show a high c-axis orientation perpendicular to the substrate, in contrast to the target used for deposition that shows all the diffraction peaks of ZnO. An example of the XRD spectrum of the thin film and target is shown in Fig. 1. No Ga_2O_3 phase was found from the XRD patterns, which implies that gallium atoms replace zinc in the hexagonal lattice and/or segregate to the noncrystalline regions located at the grain boundaries. The unit cell parameters do not vary significantly with deposition pressure and are in excellent agreement with the ZnO:Ga parameters reported in literature[13–15] with $a = 3.271$ (7) Å and $c = 5.23(1)$ Å for a film thickness of 300 nm.

According to the Scherrer formula, which calculates the crystallite size from the broadening of the (002) diffraction peak, thin films of 100 nm thickness show crystallite size ranging from 30 to 40 nm at all deposition pressures. The average crystallite size characterized by AFM is 28 nm with dispersion from 14 to 43 nm. The AFM image in Fig. 1(b) shows that the films are quite homogeneous and smooth with an arithmetic average

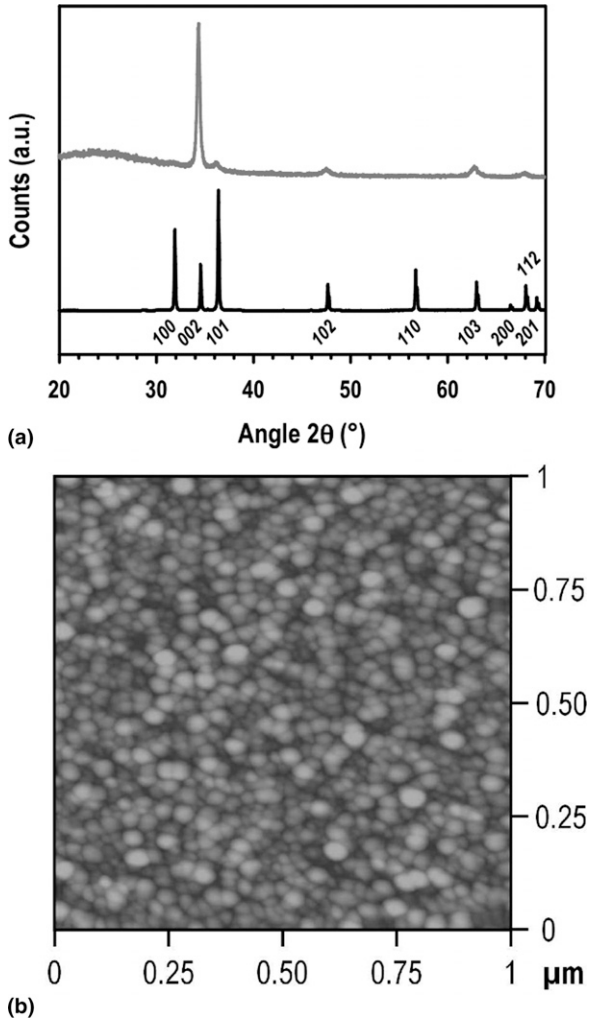

FIG. 1. (a) XRD pattern of the ZnO:Ga target (black curve) compared with the as-deposited thin film (gray curve) shows that the (002) phase is exclusively deposited. (b) AFM image of a ZnO:Ga thin film deposited at $P = 1$ Pa. The surface of the film is homogenous and smooth with an arithmetic roughness of 2 nm.

roughness (R_a) of 2 nm. The XRD-determined crystallite size is an indication of the crystallite size in the *c*-direction, i.e., into the plane of the surface since it was measured based on the (002) peak. On the other hand, AFM gives an aerial view of the crystallite size. Analyzing the XRD and AFM results together, the crystallite shape in 3D appears to have extended further in the *c*-axis than in the *x*–*y* plane, i.e., cylindrical-like structures.

Moreover, one can observe from the cross-sectional TEM images of the 100 nm samples deposited at 0.8 Pa recorded in various modes (the bright- and dark-field TEM modes, and the dark-field STEM mode) in Fig. 2 that the crystallite width is in good agreement with the XRD and AFM measurements. The Ga-doped ZnO films exhibit a columnar-type structure, evident from the TEM image in dark-field mode in Fig. 2(b). There is high orientation of the crystalline domains perpendicular to

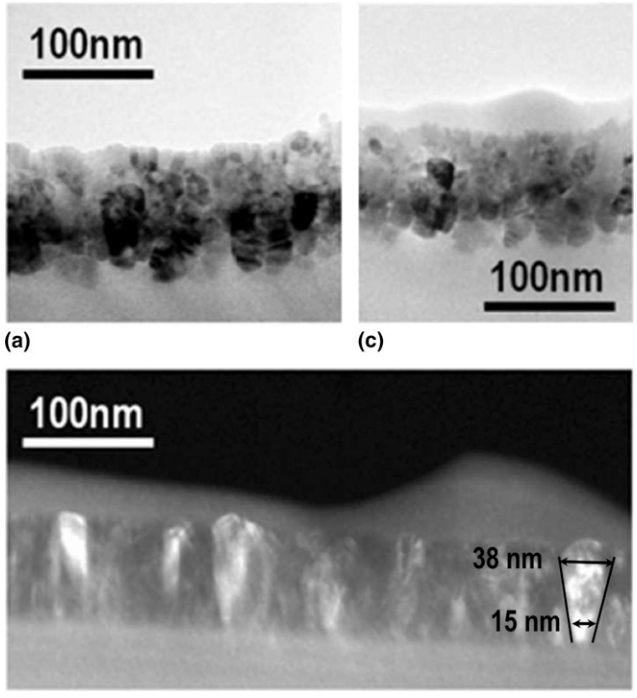

FIG. 2. Cross-sectional (a) bright-field TEM, (b) dark-field TEM, and (c) dark-field STEM micrographs of 100 nm ZnO:Ga thin film deposited at 0.8 Pa. Lines are added in (b) to highlight the conical shape of the cross section of the crystallites—the crystallites grow bigger when the thickness of the film is increased.

the substrate, in accordance with XRD results. The dark-field TEM image also indicates that the size of the coherent diffraction domain seems to increase with the film thickness as it is broad near the surface and tapers in toward the substrate.

After establishing that the crystallite size of 100 nm films does not change significantly with respect to the deposition pressure, films with various thicknesses were fabricated at the constant pressure of 0.8 Pa. With XRD, we observe that as the film thickness increases from 125 to 405 nm, the intensity of the (002) diffraction peak is enhanced. The crystallite sizes calculated from the Scherrer formula as a function of the film thickness are reported in Fig. 3. The observed full width at half-maximum becomes narrower from 0.337 to 0.223° when the film thickness increases, which can be correlated to an increase in the crystallite size from 35 to 60 nm. The thickness dependence of crystallite size is in accordance with the TEM dark-field cross-section view in Fig. 2(b). The crystallized domains increased from 15 nm at interface to 38 nm at the surface of the film. At the beginning of the deposition process, there are many nucleation centers on the substrate and for a short deposition time, small crystallites are produced. By increasing the deposition time, in other words the thickness, the crystallite size increase. This "V-shape" growth mechanism has been well described in previous works.[16,17]

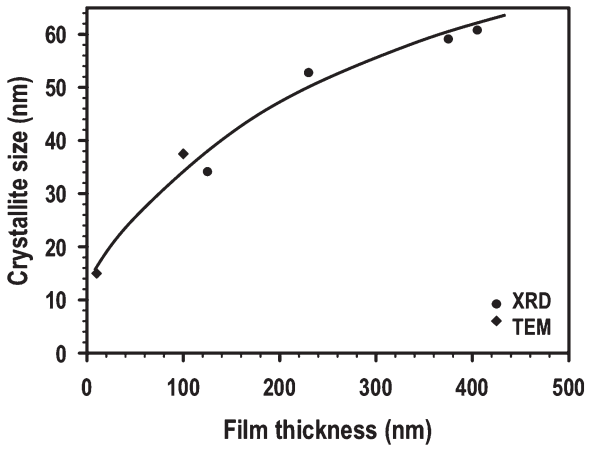

FIG. 3. Crystallite size as a function of the film thickness deposited at a constant pressure of 0.8 Pa.

The better conductivity of ZnO:Ga compared with undoped ZnO can be attributed to the nature of electrical carriers.[10] In undoped ZnO thin films, the main conductivity is due to the oxygen vacancies and zinc interstitials that bring free electrons to the conduction band. In the case of Ga-doped ZnO, besides oxygen vacancies and zinc interstitials, electrical carriers also originate from Ga^{3+} substituting Zn^{2+}. This doping mechanism contributes another free electron and leads to a higher carrier concentration in the case of ZnO:Ga.

The deposition pressure is an important factor that affects the resistivity of the as-deposited ZnO:Ga thin films: the higher the deposition pressure, the more porous will be the film.[18] At high pressure, reduced mean free paths and collision with Ar species diffracts the pathways of the incident atoms to the substrate, which results in films that are more porous, hence providing fewer conduction paths, leading to a more resistive material.[19] At the highest pressure ($P_{Ar} = 1.5$ Pa), an impoverishment of oxygen in the growing layer occurs as a result of two possible phenomena. The first is the diffusion of the oxygen during the transfer from the target to the substrate. The second is a possible reduction of the target surface due to the strong bombardment at high pressure focused by the magnetron field. The deposited thin films that are impoverished in oxygen are marked by an opposing decrease in resistivity. The resistivities of samples deposited at different pressures are listed in Table I. When the deposition pressure is increased from 0.3 to 1 Pa, the film resistivity increases as a result of the increased porosity. The decrease in resistivity at 1.5 Pa can then be attributed to the increased concentration of oxygen vacancies due to impoverishment of oxygen, which occurs in proportions that outweigh the opposing increase caused by higher porosity of the thin film at a higher deposition pressure. Another factor that affects the resistivity of the film as a result of deposition pressure is the concentration of Zn interstitials, which are discussed in more details later on. For a film deposited at $P = 0.3$ Pa, the carrier concentration and carrier mobility determined from Hall effect measurements are 1.9×10^{20} cm^{-3} and 10.9 cm^2/V · s, respectively. These values are in good agreement with literature values.[8]

TABLE I. Resistivity of ZnO:Ga thin films deposited at different pressures shows a bell-shaped effect.

Ar deposition pressure (Pa)	0.3	0.5	0.8	1.0	1.5
Resistivity ($\times 10^{-3}\ \Omega \cdot$ cm)	3.4	3	6.6	9.4	6.9

The pressure effects change the resistivity of the thin films as a result of porosity or oxygen vacancies, and in addition, even at the same pressure, the as-deposited samples show varying resistivity due to microdifferences in the deposition environment inside the chamber. This makes comparison of the samples difficult because there are too many interacting variables at the same time. Hence, we demonstrate here a method for establishing a standardized "starting point" for the samples. By subjecting the as-deposited samples to thermal treatment in vacuum, the resistivity of the film is returned to a "reference state;" hence providing a standardized platform when working with and comparing samples fabricated from different runs treated at the same condition.

Annealing in vacuum changes the concentration of several defects inside the ZnO:Ga thin film simultaneously. There are many known factors that can affect the carrier concentration and hence the resistivity of ZnO:Ga thin films when annealed under vacuum. Firstly, as mentioned briefly before, an increase in the concentration of defects such as oxygen vacancies created during the deposition process will decrease the resistivity. This is due to the reaction between oxygen vacancy and electrons in the conduction band[20] as expressed by:

$$2\,\mathrm{ZnO} \leftrightarrow 2\,\mathrm{O\,(i)} + 2\,\mathrm{Zn\,(l)} + 2\,\mathrm{O}^{\circ\circ}\mathrm{(v)} + 4\mathrm{e}^{-} \quad , \quad (1)$$

where (l) and (v) symbolizes the lattice place and vacancy, respectively. By postannealing the sample in a vacuum environment, the concentration of oxygen vacancy is further increased, which shifts the equilibrium to the right and results in further diminution of the resistivity.

On the other hand, zinc interstitial defects, which are also often created during the deposition process, will reduce the resistivity of the film by donating free electrons to the conduction band according to Eq. (2):

$$2\,\mathrm{O\,(i)} + 2\,\mathrm{Zn}^{\circ\circ}\mathrm{(i)} + 4\,\mathrm{e}^{-} \leftrightarrow 2\,\mathrm{ZnO} \quad , \quad (2)$$

where (i) represents the interstitial position. By vacuum annealing the sample, the concentration of zinc interstitial can be reduced by combining at the surface with oxygen interstitial that is created when zinc oxide is reduced [see Eq. (1)]. This phenomenon shifts the equilibrium to the right and acts to increase the resistivity. Recently, the possibility of having oxygen interstitial

diffusion has also been proposed from results of first principle calculations.[21] Diffusion of oxygen interstitial during annealing in air leads to the filling of oxygen vacancies and hence increases the resistivity of the thin film accordingly.

Another non-defect-related factor that will affect the resistivity of the thin film is the microstructure of the crystallites, which acts on the pathway of the electron carriers, rather than its concentration. Numerous small crystallites create more impedance to the pathway of electron carriers than few large crystallites over the same cross-sectional area; hence a film comprising larger crystallites will have a lower resistivity than one with smaller crystallites.

It should be highlighted that the change in microstructure and the removal of zinc interstitial are irreversible temperature-activated processes, whereas the increase/decrease in oxygen vacancies is affected by controlling both the temperature and the ambient conditions (air or vacuum) at the same time, and it is a reversible process. Hence, we note that during the first annealing cycle, a mixture of effects arising from the removal of zinc and oxygen interstitials, creation of oxygen vacancies, and change in microstructure will be observed. After the first vacuum annealing, the effects arising from the filling/creation of oxygen vacancies are exclusively observed during subsequent annealing cycles. This will distinguish the effect of oxygen vacancies from the rest of the parameters.

Adopting this method of vacuum annealing as a platform for comparison of samples deposited at different pressures, an interesting observation was made when comparing the difference between the "as-deposited" resistivity and the "reference state" resistivity of samples deposited at different pressures. Figure 4 shows the resistivity versus temperature measurements performed first in vacuum, and then in air for four samples deposited at 0.3, 0.5, 0.8, and 1 Pa. The stand-alone points mark the as-deposited resistivity for each sample, and the arrows indicate the direction of change in resistivity after the first vacuum annealing, thereby arriving at the "reference starting point" of each sample. Subsequent annealing and cooling in air results in a change of the resistivity as can be traced by the cyclic curves. In Fig. 4(b), the percentage change in as-deposited resistivity at each deposition pressure expressed as a function of the "reference starting point" is illustrated. For the cycling curve at 0.5 Pa, the data points between 150 and 200 °C are deleted because of systematic disturbance to the signal as a result of noise during the electrical measurement. This region is marked with a solid line for visual guide.

For the thin films deposited at 0.5, 0.8, and 1.0 Pa, the resistivity of the as-deposited samples is lowered by 70%, 45%, and 91%, respectively, after annealing in vacuum at 400 °C as illustrated in Fig. 4. This is an

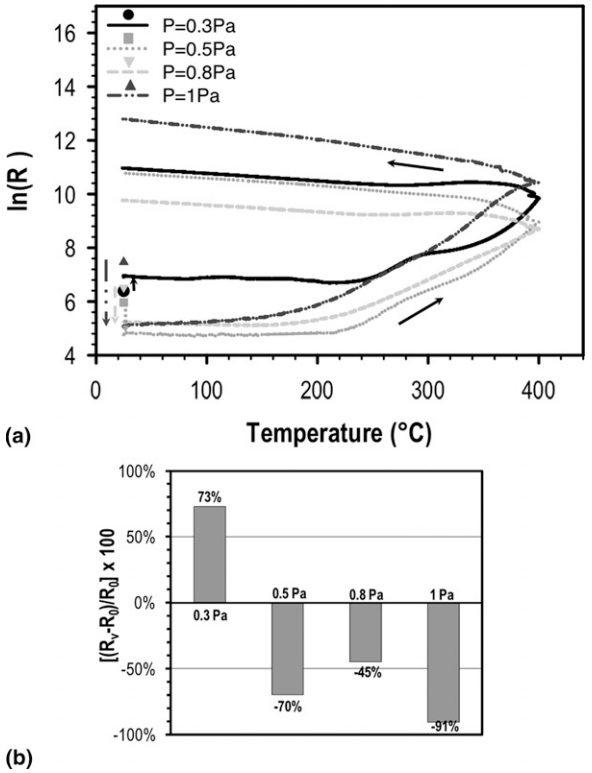

FIG. 4. Resistivity versus temperature measurements performed first in vacuum, and then in air for four samples deposited at 0.3, 0.5, 0.8, and 1 Pa. The stand-alone points mark the as-deposited resistivity for each sample, and the arrows indicate the direction of change in resistivity after the first vacuum annealing, thereby arriving at the "reference starting point" of each sample. Subsequent annealing and cooling in air results in a change of the resistivity as can be traced by the cyclic curves. In the inset, the percentage change in resistivity of each deposition pressure expressed as a function of the "reference starting point" is illustrated. R_o is the as-deposited resistivity, while R_v is the resistivity after the first vacuum annealing. For the cycling curve at 0.5 Pa, the data points between 150 and 200 °C are deleted due to systematic disturbance to the signal as a result of noise during the electrical measurement. This region is marked with a solid line for visual guide.

expected behavior due to the creation of oxygen vacancies.[11,20,22] In contrast, for the thin films deposited at 0.3 Pa, the resistivity is increased by 73% after annealing in vacuum, which is rather unexpected. The three main factors that change with annealing in vacuum are oxygen vacancy, zinc interstitial, and microstructure, as already discussed. For the samples deposited at 0.3 Pa, atoms arrive from the target onto the substrate with a large mean free path; they do not undergo many collisions and do not lose energy in the process. Even if the mean energy of sputtered species is around a few electronvolts, the energy distribution of these particles adopts values ranging between less than 1 eV and few tens of eV. Therefore, some particles keep an energy that allows implantation through just a few angstroms under the surface of the growing layer. Another effect that arises from the Ar atoms (reflected from the target) that bombard the

surface of the growing layer with high energy is the ability to create atomic displacement into the crystal lattice. This implants a lot of defects into the thin film, resulting in a higher concentration of zinc interstitial defects. In addition, films deposited at this condition are compact and relatively flat (i.e., nonporous) because the incident atoms follow a relatively straight pathway from the target to the substrate. Consequently, during vacuum annealing, there exist few accessible surface areas for the creation of more oxygen vacancies, but plenty of implanted zinc interstitial defects available for removal. The effect of zinc interstitials removal outweighs that of the oxygen vacancies creation, which explains why the resistivity was increased for the sample deposited at 0.3 Pa. In contrast, for samples deposited at higher pressures of 0.5, 0.8, and 1.0 Pa, the diffused pathways of the incident atoms to the substrate creates films that are more porous and with rougher surfaces. This provides a high density of accessible sites for the creation of more oxygen vacancies during vacuum annealing. At the same time, fewer implanted zinc interstitials are created during high-pressure deposition due to energy loss from collisions as a result of the short mean free path of the incident atoms. Consequently, the effect of oxygen vacancy creation outweighs the opposing effect of reducing the concentration of zinc interstitials during vacuum annealing, hence decreasing the overall resistivity. After the first (vacuum) annealing at 400 °C, the 300 nm sample deposited at 0.8 Pa was found to show a small increase in crystallite size from 43 to 48 nm when studied by AFM and from 67 to 100 nm when studied by XRD. Hence, the enlargement of crystallite size during annealing is another factor that results in a decrease in the resistivity of the sample during the first annealing cycle. Subsequent annealing results in no change in crystallite size.

The oxygen stoichiometry is a critical parameter for the electrical properties of ZnO:Ga thin films. As we have seen, it can be adjusted by the deposition conditions and also postdeposition annealing treatments.[10] The reversibility of resistivity during annealing treatment in vacuum and air is shown in Fig. 5, for the sample deposited at 1 Pa. This trend has also been observed on samples deposited at other pressures. After vacuum annealing at 400 °C, the electrical resistivity of ZnO:Ga thin films decreases, as marked by the arrow starting from the stand-alone point (as-deposited resistivity) to the start of the black curve. Annealing in vacuum can eliminate oxygen in the thin film from three places: surface, pores, and/or between grain boundaries.[22] The partial removal of oxygen atoms from the thin film creates oxygen vacancies, hence improving the conduction. By annealing the same sample in air at 400 °C, the electrical resistance can be increased to a value higher than the as-deposited sample, as traced by the black curve. Below 200 °C, the increase in resistivity is not significant.

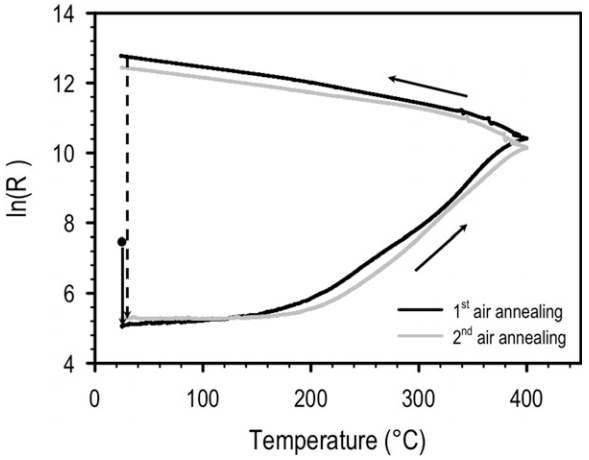

FIG. 5. Resistivity versus temperature measurement for a sample deposited at 1 Pa. Cyclic annealing of the as-deposited sample in vacuum results in a decrease in resistivity from the stand-alone point to the point as marked by the arrow. Subsequent annealing and cooling in air led to a change in resistivity as traced by the black curve. When vacuum annealing is repeated, the resistivity drops again as marked by the broken arrow, and repeated annealing/cooling in air again cycle the resistivity as traced by the gray curve. This shows the reversibility of oxygen vacancy creation/filling in the ZnO:Ga thin film.

However, above this temperature and up to 400 °C, oxidation takes place and the resistivity increased by 2 orders of magnitude, due to the filling of oxygen vacancies. This shows that it is a temperature-activated process. Figure 5 shows that after the first cyclic treatment, the oxygen vacancies can again be created by annealing the same sample in vacuum to yield the same resistivity minimum, as illustrated by the broken arrow. These vacancies can subsequently be filled by air annealing treatment (gray curve), fully illustrating the cyclicality of the process. The lowest obtained resistivity is about $2.5 \times 10^{-3}\ \Omega \cdot \mathrm{cm}$ after vacuum annealing at 400 °C for 1 h.

As illustrated in these examples, samples that have already been tested can have their defects "reset" to their reference starting point by annealing in vacuum. This allows re-experimentation of the same sample after several runs because by annealing in vacuum at 400 °C, the resistivity value will return to the reference starting point. As long as the treatment temperature is not higher than 400 °C, the crystallite size of the thin films will not change with repeated annealing. Similarly, when comparing several samples deposited at the same conditions, variations in resistivity as a result of minor variations during deposition can be corrected to its reference starting point as a platform for standardizing the "starting conditions" of the samples. This allows more control over the experiments as one can always easily return to the "starting point" at any stage during the experiments. This advantage also applies in the case of studying samples deposited with different pressures because changing the deposition pressure leads to multiple opposing effects

on the resistivity of the samples as presented previously, and by vacuum annealing, samples deposited at different conditions are corrected to a different reference starting point unique to the deposition condition. Vacuum annealing also opens up a larger window for studying the effect of oxygen vacancies on the samples. In contrast, the effect of microstructure can be distinguished by performing air annealing instead of vacuum annealing as the first annealing step. These annealing studies serve only the objective of understanding the relationship between defects and electrical properties. It does not withdraw the interest of the rf sputtering as one of the most appropriate techniques for the deposition on polymer substrates at low temperature.

For a sample deposited at $P = 0.5$ Pa and with thickness to 100 nm, the average transmittance is about 87% in the range from 400 to 800 nm. The optical absorption coefficient α of a semiconductor with a direct band gap is given by[14]

$$(\alpha \cdot h\nu)^2 = A(h\nu - E_g) \quad ,$$

where A is a constant, $h\nu$ is the photon energy, and E_g is the optical energy band gap. Thus, the optical band gap E_g can be calculated by estimating the α values at each wavelength using the transmittance spectra, followed by plotting $(\alpha h\nu)^2$ versus $h\nu$ (figure not shown). Extrapolating the linear portion of this plot and taking the intercept of the data line with the energy axis gives the value of E_g. The optical band gap for this ZnO:Ga film is estimated to be 3.38 eV, which is in line with the results obtained by Gomez et al.,[23] who found the energy band gap varying from 3.28 to 3.32 eV for ZnO:Ga (2 at.%) films with a thickness of 600 nm.

IV. CONCLUSION

ZnO:Ga thin films were deposited by nonreactive rf-magnetron sputtering on conventional glass substrates at room temperature. X-ray diffraction studies show that all the ZnO:Ga films crystallized with the hexagonal wurtzite structure and were highly oriented along the crystallographic *c*-axis perpendicular to the substrate. Structural analysis proved that as the film thickness increases, the grain size becomes larger. The effects of annealing on the electrical properties of ZnO:Ga thin films were investigated as a function of the deposition pressure. The final resistivity of the film is largely governed by the opposing effects of zinc interstitial and oxygen vacancy defect density and the microstructure during annealing, which in turn can be varied with the deposition pressure. We propose a methodology of using vacuum annealing to create a standardized platform for comparing samples deposited with different conditions by "resetting" the resistivity to a reference point where all intrinsic defects are at its minimum or maximum. Beyond the first annealing treatment, annealing under vacuum works to decrease the resistivity due exclusively to the creation of oxygen vacancies, while annealing in air has the opposite effect. Subsequent annealing of the sample under air and vacuum showed that the process is reversible and cyclable. The average transmittance of all ZnO:Ga thin films was more than 87% in the visible range.

ACKNOWLEDGMENT

J.M. Soon would like to thank the Foundation of Sciences et Technologies pour l'Aéronautique et l'Espace (STAE) for funding this work under the project "Systèmes miniaturisés intelligents pour l'aéronautique et l'espace" (SYMIAE).

REFERENCES

1. Ü. Özgür, Ya.I. Alivov, C. Liu, A. Teke, M.A. Reshchikov, S. Doğan, V. Avrutin, S-J. Cho, and H. Morkoç: A comprehensive review of ZnO materials and devices. *J. Appl. Phys.* **98,** 041301 (2005).
2. M. Berginski, J. Hüpkes, W. Reetz, B. Rech, and M. Wuttig: Recent development on surface-textured ZnO:Al films prepared by sputtering for thin-film solar cell application. *Thin Solid Films* **516**(17), S5836 (2008).
3. B-Y. Oh, M-C. Jeong, T-H. Moon, W. Lee, J-M. Myoung, J-Y. Hwang, and D-S. Seo: Transparent conductive Al-doped ZnO films for liquid crystal displays. *J. Appl. Phys.* **99,** 124505 (2006).
4. T. Minami, T. Miyata, and Y. Ohtani: Optimization of aluminum-doped ZnO thin-film deposition by magnetron sputtering for liquid crystal display applications. *Phys. Status Solidi. A* **204**(9), 3145 (2007).
5. ZnO and related materials. *Superlattices and Microstructures* **42,** 1 (2007).
6. B.G. Lewis and D.C. Paine: Applications and processing of transparent conducting oxides. *MRS Bull.* **15,** 22 (2000).
7. E. Fortunato, A. Gonçalves, V. Assunção, A. Marques, H. Águas, L. Pereira, I. Ferreira, and R. Martins: Growth of ZnO:Ga thin films at room temperature on polymeric substrates: Thickness dependence. *Thin Solid Films* **442,** 121 (2003).
8. V. Assunção, E. Fortunato, A. Marques, H. Águas, I. Ferreira, M.E.V. Costa, and R. Martins: Influence of the deposition pressure on the properties of transparent and conductive ZnO:Ga thin-film produced by r.f. sputtering at room temperature. *Thin Solid Films* **427,** 401 (2003).
9. X. Yu, J. Ma, F. Ji, Y. Wang, X. Zhang, C. Cheng, and H. Ma: Effects of sputtering power on the properties of ZnO:Ga films deposited by r.f. magnetron-sputtering at low temperature. *J. Cryst. Growth* **274,** 474 (2005).
10. K. Yim and C. Lee: Dependence of the electrical and optical properties of sputter-deposited ZnO:Ga films on the annealing temperature, time, and atmosphere. *J. Mater. Sci. Mater. Electron.* **18,** 385 (2007).
11. S. Major, A. Banerjee, and K.L. Chopra: Annealing studies of undoped and indium doped films of zinc oxide. *Thin Solid Films* **122,** 31 (1984).
12. K.H. Kim, K.C. Park, and D.Y. Ma: Structural, electrical and optical properties of aluminum doped zinc oxide films prepared by radio frequency magnetron sputtering. *J. Appl. Phys.* **81**(12), 7764 (1997).

13. K. Wasa, M. Kitabatake, and H. Adachi: *Thin Film Materials Technology—Sputtering of Compound Materials* (Springer, William Andrew Publishing, New York, 2004).
14. N.R. Aghamalyan, E.A. Kafadaryan, R.K. Hovsepyan, and S.I. Petrosyan: Absorption and reflection analysis of transparent conductive Ga-doped ZnO films. *Semicond. Sci. Technol.* **20,** 80 (2005).
15. A. de Souza Gonçalves, S.A. Marques de Lima, M.R. Davolos, S.G. Antonio, and C. de Oliveira Paiva-Santos: The effects of $ZnGa_2O_4$ formation on structural and optical properties of ZnO: Ga powders. *J. Solid State Chem.* **179,** 1330 (2006).
16. X. Yu, J. Ma, F. Ji, Y. Wang, C. Cheng, and H. Ma: Thickness dependence of properties of ZnO:Ga films deposited by rf magnetron sputtering. *Appl. Surf. Sci.* **245,** 310 (2005).
17. M. Bouderbala, S. Hamzaoui, B. Amrani, A.H. Reshak, M. Adnane, T. Sahraoui, and M. Zerdali: Thickness dependence of structural, electrical and optical behaviour of undoped ZnO thin films. *Physica B* **403,** 3326 (2008).
18. F. Oudrhiri-Hassani, L. Presmanes, A. Barnabé, and P. Tailhades: Microstructure and roughness of RF sputtered oxide thin films: Characterization and modelization. *Appl. Surf. Sci.* **254,** 5796 (2008).
19. S. Capdeville, P. Alphonse, C. Bonningue, L. Presmanes, and P. Tailhades: Microstructure and electrical properties of sputter deposited $Zn_{0.87}Fe_{2.13}O_4$ thin layers. *J. Appl. Phys.* **96**(11), 6142 (2004).
20. K. Ellmer: Electrical properties, in *Transparent Conductive Zinc Oxide—Basics and Applications in Thin Film Solar Cells*, edited by K. Ellmer, A. Klein, and B. Rech (Springer, 2008), p. 35.
21. G-Y. Huang, C-Y. Wang, and J-T. Wang: First-principles study of diffusion of oxygen vacancies and interstitials in ZnO. *J. Phys. Condens. Matter* **21**(19), 195403 (2009).
22. K.Y. Cheong, N. Muti, and S.R. Ramanan: Electrical and optical studies of ZnO:Ga thin films fabricated via the sol-gel technique. *Thin Solid Films* **410,** 142 (2002).
23. H. Gomez, A. Maldonado, M. de la L. Olvera, and D.R. Acosta: Gallium-doped ZnO thin films deposited by chemical spray. *Sol. Energy Mater. Sol. Cells* **87,** 107 (2005).